MODIS Collection 6.1 3 km resolution aerosol optical depth product: global evaluation and uncertainty analysis

Jing Wei [a,b,*], Zhanqing Li [b,**], Lin Sun [c], Yiran Peng [d], Lei Liu [e], Lijie He [f], Wenmin Qin [g], Maureen Cribb [b]

[a] State Key Laboratory of Remote Sensing Science, College of Global Change and Earth System Science, Beijing Normal University, Beijing, China
[b] Department of Atmospheric and Oceanic Science, Earth System Science Interdisciplinary Center, University of Maryland, College Park, MD, USA
[c] College of Geodesy and Geomatics, Shandong University of Science and Technology, Qingdao, China
[d] Ministry of Education Key Laboratory for Earth System Modeling, Department of Earth System Science, Tsinghua University, Beijing, China
[e] College of Earth and Environmental Sciences, Lanzhou University, Lanzhou, China
[f] Department of Geography and Resource Management, The Chinese University of Hong Kong, Shatin, Hong Kong, China
[g] School of Geography and Information Engineering, China University of Geosciences, Wuhan, China

HIGHLIGHTS

- MODIS Collection 6.1 3 km resolution AOD products are evaluated globally.
- The accuracy has been improved overall after data quality control.
- Retrievals errors related to varying surface and atmospheric conditions are analyzed.
- MODIS 3 km DT AOD product is generally less accurate than the 10 km DT release.

ARTICLE INFO

ABSTRACT

Recently, NASA has released the newest Moderate Resolution Imaging Spectroradiometer (MODIS)/Terra Collection 6.1 (C6.1) aerosol product generated at a higher spatial resolution of 3 km (i.e., MOD04_3K) with main updates in the radiation calibration and the Dark Target (DT) aerosol algorithm. This product is of great importance for air pollution studies at small to medium scales but has not been fully evaluated. This paper aims to provide a comprehensive validation and error analysis of the MOD04_3K C6.1 aerosol optical depth (AOD) data set against Aerosol Robotic Network (AERONET) Version 3 AOD measurements at different spatiotemporal scales from 2013 to 2017 over land and ocean. Results suggest that the data quality of the MOD04_3K AOD data set is overall improved at different spatial scales after quality control. In general, the highest-quality 3 km AOD retrievals (quality assurance = 3) and ground-based measurements are highly correlated (correlation coefficient = 0.81), with a mean absolute error of 0.08 and a root-mean-square error of 0.12. About 63% of the data samples fall within the expected error envelope on a global scale. Nevertheless, there is large spatial heterogeneity in the performance at regional and site scales, with the worse accuracy generally observed in areas covered by bright surfaces or dominated by human activities. This is mainly due to the difficulties in estimating surface reflectance and the aerosol-type assumption. In addition, aerosol retrievals are overall overestimated, especially over North America, Europe, and East Asia. Furthermore, the estimation errors and uncertainties are highly related to varying surface and atmospheric aerosol conditions, which become larger with increases in surface brightness, aerosol loading, Ångström exponent and single scattering albedo. The MODIS 3 km AOD data set is generally less accurate than its coarser-spatial-resolution (10 km) counterpart due to a decrease in the opportunity to discard marginal pixels from the retrieval. Therefore, further algorithm improvements are needed to reduce the estimation uncertainty, especially for heterogeneous urban and bright surfaces.

---

* Corresponding author.
** Corresponding author.
  E-mail addresses: weijing_rs@163.com (J. Wei), zli@atmos.umd.edu (Z. Li).

1. Introduction

Atmospheric aerosol particles have important effects on Earth's radiative balance by directly absorbing and scattering solar radiation (Charlson et al., 1992; Haywood and Boucher, 2000; Li et al., 2017a; Qin et al., 2020; Yu et al., 2006; Zeng et al., 2019) and by affecting the optical properties and lifetimes of clouds (Haywood and Boucher, 2000; Koren et al., 2012; Li and Coauthors, 2017b; Oreopoulos et al., 2016; Su et al., 2018, 2020). In particular, fine particles can damage human health, arousing much public concern (Bartell et al., 2013; Peng et al., 2009; Wei et al., 2019a, b, 2020). Aerosol optical depth (AOD) refers to the integration of the extinction coefficient of the atmosphere in the vertical direction, a key quantitative physical quantity characterizing the degree of atmospheric turbidity. Nowadays, ground-based aerosol monitoring networks have been established to monitor air pollution in real-time. However, aerosols show great spatiotemporal variations. Since these ground stations are sparsely distributed, it is difficult to meet the needs of wide-scale monitoring.

Satellite remote sensing technology can overcome this issue and obtain AODs based on a variety of aerosol retrieval algorithms (Kaufman et al., 1997). An increasing number of satellite sensors have released their own official aerosol products. These products are generated from different aerosol retrieval algorithms, and most of them are produced at coarse spatial resolutions that are difficult to satisfy the requirements of air pollution monitoring at small to medium scales. Among them, the Moderate-resolution Imaging Spectroradiometer (MODIS) aerosol product has become more popular in related applications due to their longer data records starting from the beginning of the twenty-first century and more mature aerosol retrieval algorithms. Besides the popular 10 km resolution aerosol product, a global-coverage daily MODIS aerosol product at a higher spatial resolution of 3 km has recently been released (Remer et al., 2013). Due to its much higher spatial resolution, it has been used in multiple air pollution related studies, including the investigation of spatiotemporal aerosol variations and the estimation of fine particulate matter concentrations (Ma et al., 2017; Munchak et al., 2013; Xue et al., 2019).

The MODIS 3 km aerosol product is generated based on the second-generation operational Dark Target (DT) algorithm. The same algorithm is used to generate the MODIS 10 km aerosol product, which includes the same surface reflectance estimation, aerosol-type assumption, look-up-table construction, and unsuitable-pixel screening. The main differences between the two retrievals are the size of the aggregation window and the number of pixels needed in the aerosol retrieval box. The 10 km aerosol retrieval begins with a spatial window of 20×20 pixels, while the 3 km aerosol retrieval uses a narrower spatial window of 6×6 pixels. After removing unsuitable pixels, the remaining pixels are first sorted, and then 20% and 50% of the darkest and brightest pixels, respectively, are removed. This leaves twelve or fewer pixels, with a limited minimum of 5 pixels required in the 3 km retrieval box. This means that the pixels used in the 3 km retrieval box would possibly be discarded in the coarser 10 km retrieval box. The reflectance of the remaining pixels is then averaged and used for aerosol retrieval (Gupta et al., 2018; Remer et al., 2013).

An increasing number of studies have evaluated the MODIS 3 km aerosol product at national and global scales (Gupta et al., 2018; He et al., 2017; Nichol and Bilal, 2016; Remer et al., 2013). Among them, Gupta et al. (2018) provided a comprehensive validation of MODIS Collection 6 (C6) 3 km AODs against AErosol RObotic NETwork (AERONET) Version 3 AOD measurements over land. They found that the accuracy of the 3 km retrieval varied locally and regionally, even differing among spatially continuous sites. The accuracy was significantly degraded when involving poor-data-quality retrievals in the analysis, and appeared to be less accurate than 10 km retrievals on a global scale. The error dependencies on AOD loading and geometry suggest that greater errors might arise from uncertainties in pixel selection and the assumption of surface and aerosol characteristics.

On March 7, 2018, the MODIS C6 3 km aerosol product was updated to C6.1 with further calibration corrections and a series of improvements in the DT aerosol algorithm. The forward-stream processing of C6 ended in April 2018. Different from the C6 release, the C6.1 release was generated from the updated Level 1B calibrated radiance product with additional corrections in radiometric calibration (Jeong et al., 2011; Meister et al., 2014). In addition, several main algorithm updates were made, including 1) added quality control in reflectance, cloud fraction, and the number of effective pixels, and a modified sediment mask over oceans; 2) updated data quality control for coastal and water conditions; 3) improved surface reflectance estimations over urban areas (Gupta et al., 2016); and 4) many other aspects, such as bug fixes and the removal of a few redundant subroutines (https://atmosphere-imager. gsfc.nasa.gov/sites/default/files/ModAtmo/C061_Aerosol_Dark_Target _v2.pdf). Given the continual refinements in both data records and the aerosol retrieval algorithm, the newly released MODIS C6.1 3 km aerosol product has not been fully evaluated, and the performance of this product is still unclear on a global bias.

This study, therefore, aims to provide a comprehensive global validation of the latest MODIS C6.1 3 km resolution AOD data set against the newest AERONET Version 3 AOD measurements over both land and ocean, as well as their estimation errors and uncertainties related to varying surface characteristics and atmospheric aerosol conditions. Their overall accuracy with reference to the MODIS C6.1 10 km coarser resolution aerosol product and spatiotemporal characteristics are also investigated. Section 2 describes the satellite remote sensing and ground-based data and introduces the evaluation and analysis approaches. Section 3 presents the validation results, uncertainties, and comparisons of aerosol products, and investigates the spatial distributions and variations over land and ocean. Section 4 summarizes the main conclusions.

2. Data and methods

2.1. Satellite remote sensing products

In this study, only the MODIS/Terra Level 2 daily swath AOD data set at a spatial resolution of 3 km (i.e., MOD04_3K) are selected for evaluation. The MODIS/Aqua AOD data set (i.e., MYD04_3K) is not considered here because the same retrieval algorithm is used to generate AODs, showing the similar overall accuracy. Differences between the two retrievals may be caused by the different characteristics of the sensors, such as different imaging times, sensor lifetimes, and sensor degradation (Bright and Gueymard, 2019; Fan et al., 2017; Gupta et al., 2018). The MODIS 3 km aerosol product provides a Quality Assurance (QA) data set to indicate the quality confidence of the aerosol retrievals. This quality control is comprised of several tests regarding water and bright surfaces, possible (cirrus) clouds, fitting errors, and sufficient numbers of data samples during the retrieval process (Levy et al., 2013; Wei et al., 2018a).

MODIS/Terra has recorded data for more than 20 years. However, the main purpose of this study is to quantitatively evaluate the overall accuracy and uncertainty of the MOD04_3K aerosol product, not explore long-term aerosol variations. To save on storage and processing time, only about a quarter of the MODIS/Terra records (from 2013 to 2017) is selected here. All possible retrievals (QA = All) and the highest-quality (QA = 3) AOD retrievals at 550 nm over land and ocean from 2013 to 2017 are employed for validation purpose. The MODIS/Terra C6.1 Level 2 daily AOD data set at a coarser 10 km resolution (i.e., MOD04_L2) covering the same period are collected for comparison, and only those DT AOD retrievals at 550 nm having the highest quality (QA = 3) are used. The MODIS/Terra C6.1 Level 3 monthly aerosol product (i.e., MOD08_M3) covering the same study period is also employed to analyze global spatiotemporal aerosol characteristics. Furthermore, several auxiliary remote sensing products are also selected to assist in analyzing the estimation error and uncertainty, and then they are resampled to a

uniform spatial resolution of 0.03 ° × 0.03 ° to be consistent with the MOD04_3K product. Table 1 summarizes all satellite remote sensing products used in this study.

2.2. AERONET AOD measurements

Widely used AERONET measurements are selected to evaluate the MODIS aerosol product, providing instantaneous aerosol spectral measurements at multiple wavelengths (e.g., 440, 500, 675, 870, and 1020 nm) every 15 min (Holben et al., 1998). The newest Version 3 Level 2.0 (cloud screened and quality assured) AOD and Ångström exponent (AE, 440–675 nm) measurements, and single scattering albedo (SSA) retrievals are employed (Giles et al., 2019). This study uses data from 384 globally distributed AERONET sites (Fig. 1) with more than one year of data records, including 350 sites located on land and 34 sites surrounded by ocean (mainly distributed in offshore seas). Here, MODIS aerosol products are validated against AERONET measurements at land and ocean sites separately, as well as in ten continental regions of interest. There are 98 sites in Europe (EUR), 62 sites in eastern North America (ENA), 47 sites in western North America (WNA), 36 sites in East Asia (EAA), 27 sites in South America (SAM), 29 sites in North Africa and the Middle East (NAM), 20 sites in Southeast Asia (SEA), 13 sites in South Africa (SAF), 10 sites in South Asia (SAA), and 8 sites in Oceania (OCE).

2.3. Evaluation and analysis methods

Since AERONET does not provide AOD measurements at 550 nm, instead of using the Ångström algorithm approach (Sun et al., 2016a; Wei et al., 2019c), the more robust second-order polynomial fit approach (Eq. (1)) is selected to interpolate the 550-nm AOD based on the measurements at 870, 675, 500, and 440 nm (Sayer et al., 2019; Schuster et al., 2006):

$$\log(\tau_{550}) = a_0 \log(550) + a_1 \log(550)^2 + b, \tag{1}$$

where τ is the AOD at 550 nm, and a_0, a_1, and b are regression coefficients.

For spatiotemporal matching, an AOD retrieval is defined as the average value of all available MODIS pixels falling within the latitude/longitude sampling window of 0.15 ° × 0.15 ° centered on each AERONET station (Gupta et al., 2018). The real AOD value is defined as the average value of at least two AERONET AOD measurements within ±30 min of the satellite overpass time (Gupta et al., 2018; Wei et al., 2019c). In this study, the following statistical metrics are selected to quantitatively evaluate the consistency and uncertainty between MODIS and AERONET AOD retrievals: the correlation coefficient (R), the mean bias, the mean absolute error (MAE), the root-mean-square error (RMSE), and the relative mean bias (RMB).

The expected error (EE) envelope, representing the percentages (or fractions) of the AOD retrievals falling within/above/below the custom error range, is calculated as

$$EE = \pm (0.05 + 0.15 * \tau_{AERONET}). \tag{2}$$

Note that this EE was determined from the MODIS 10 km DT product over land (Levy et al., 2010, 2013), which is not based on any analysis of the 3 km release offered by the DT development team. This EE envelope is stricter that what was found in C6 (Gupta et al., 2018; Remer et al., 2013).

The relative difference (RD, %) of each statistical metric between MODIS 3 km and 10 km AOD retrievals (Wei et al., 2019d) is calculated as

$$RD = [(M_{3km} - M_{10km})/M_{10km}] * 100\%, \tag{3}$$

where M is the statistical metric in question.

For the spatiotemporal analysis, spatial coverage (%) is defined as the proportion of effective AOD retrievals of the MODIS aerosol product in space. Monthly and seasonal spatial coverages are calculated using the area-weighting approach (Wei et al., 2019e). In addition, MOD08 monthly AOD maps are averaged for each grid to generate seasonal AOD maps for each year, used to show the spatiotemporal coverage and distribution of the MODIS aerosol data set. Here, only the global spatial coverage and distribution on monthly and seasonal bases are evaluated because there are numerous missing aerosol retrievals on a daily basis due to cloud contaminations. Monthly or seasonal spatial coverages and distributions of AOD products are useful because such information is potentially important for related aerosol studies such as aerosol algorithm development, long-term aerosol variations, and climate model simulations or predictions.

3. Results and discussion

3.1. Validation against surface measurements

3.1.1. Global-scale performance

Collocated were a total number of 90,667 all-quality AOD retrievals (QA = All) from 2013 to 2017 at all available 370 sites around the world. Satellite- and ground-based retrievals agree well (R = 0.79), with an average MAE of 0.08 and an RMSE of 0.13 (Fig. 2a). However, many AOD retrievals are overestimated (RMB = 2.05), with ~37% of the matchups falling above the EE envelope. There are 81,721 and 8946 all-quality AOD matchups collocated at 350 land and 34 ocean AERONET sites (Fig. 2b–c). The range of AOD loading over land is about three times greater than that over oceans. This is because, aside from urban and industrial aerosols, land is the source of dust aerosols, which is the largest particle constituent by mass, and emissions from natural wildfires, which is the single largest aerosol constituent in North America, Australia, and the boreal forests of Asia. About 60% of the matchups fall within the EE envelope. However, land AOD retrievals have overall larger estimation uncertainties than coastal AOD retrievals. The main reasons are that the land surface includes a variety of land-cover types with varying surface reflectances, and the sources and components of aerosols vary greatly over space and time.

After data quality control, the total number of highest-quality AOD matchups (QA = 3) decreased by 10%, 11%, and 7% during 2013–2017 over the globe, land, and ocean, respectively (Fig. 2d–f). More
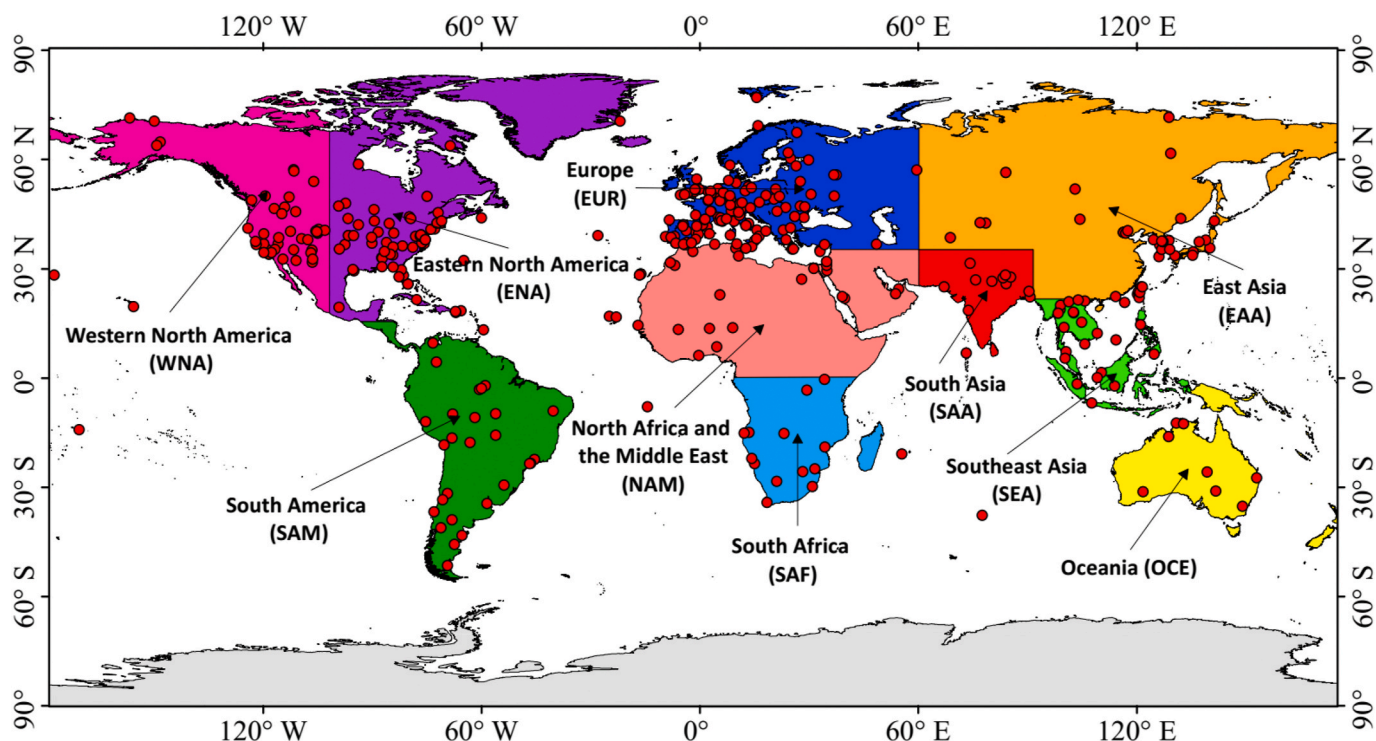
Table 1
Satellite remote sensing products used in this study.

Product	Content	Scientific Data Set	Spatial resolution	Temporal resolution
MOD04_3K	DT AOD (QA = 3)	Image_Optical_Depth_Land_And_Ocean	3 km	Daily
	DT AOD (QA = All)	Optical_Depth_Land_And_Ocean		
	Aerosol type	Aerosol_Type_Land		
MOD04_L2	DT AOD (QA = 3)	Optical_Depth_Land_And_Ocean	10 km	Daily
MOD08_M3	DT AOD (Corrected)	Aerosol_Optical_Depth_Land_Ocean_Mean_Mean	1 ° × 1 °	Monthly
MOD09A1	Surface reflectance	sur_refl_b03 (459–479 nm)	500 m	8-day
MCD12C1	Land cover type	Land Cover Type 1	0.05 ° × 0.05 °	Yearly
MOD13C2	NDVI	NDVI	0.05 ° × 0.05 °	Monthly
STRM	Elevation	DEM	90 m	–

DEM: digital elevation model; NDVI: normalized difference vegetation index; STRM: Shuttle Radar Topography Mission.

Fig. 1. Locations of AERONET sites (red dots) and the ten continental regions of interest (different colored areas) defined according to our previous study (Wei et al., 2019c). (For interpretation of the references to color in this figure legend, the reader is referred to the Web version of this article.)
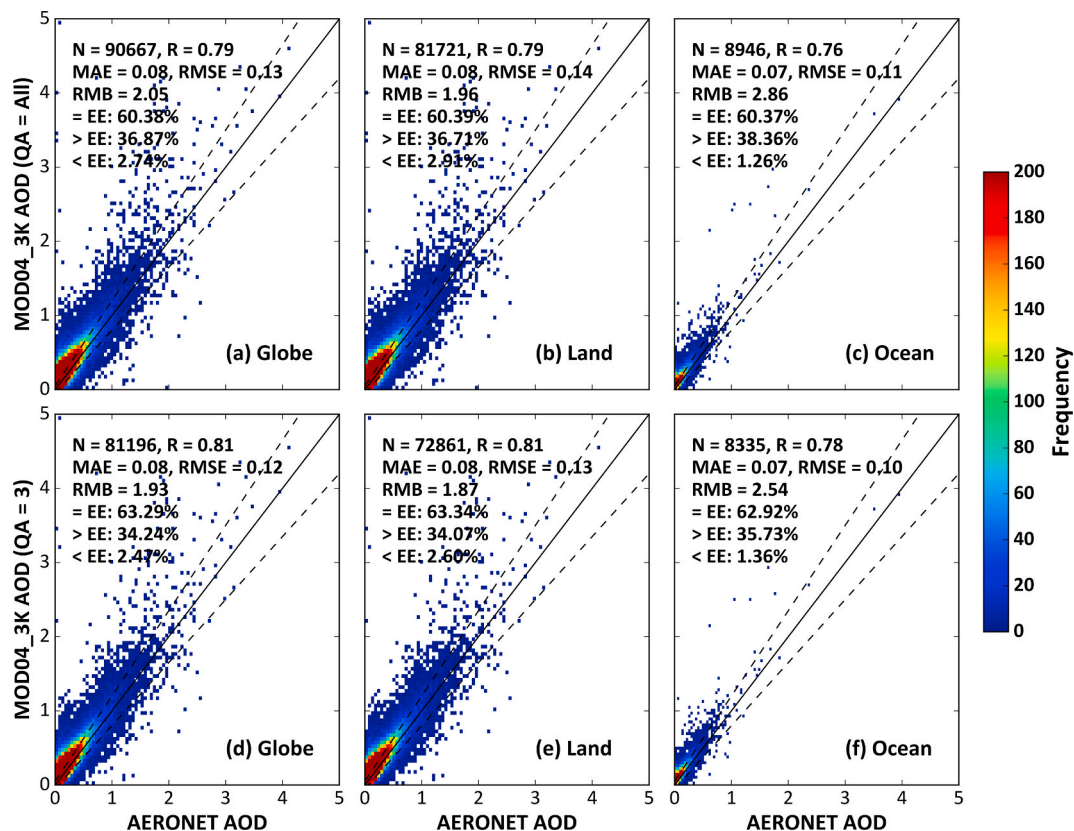

Fig. 2. Density scatter plots of MODIS/Terra 3 km (a–c) all-quality (QA = All) and (d–f) highest-quality (QA = 3) AOD retrievals as a function of AERONET AODs over the globe, land, and ocean from 2013 to 2017. The solid line denotes the 1:1 line, and the dashed lines denote the expected error (EE) envelope. Note that " = EE", "> EE", and "< EE" show the percentages (%) of retrievals falling within, above, and below the EE envelope, respectively.

importantly, the overall accuracy improved, with increasing correlations and decreasing RMSE and RMB values. Overall, the number of matchups falling within the EE envelope over the globe, land, and ocean increased to 63.29%, 63.34%, and 62.92%, respectively. However, many AOD retrievals are still overestimated (RMB = 1.8–2.6). This suggests that MOD04_3K AOD retrievals passing the highest data quality (QA = 3) should be used for aerosol-related studies, which was also the recommendation of the NASA team (Gupta et al., 2018).

3.1.2. Continent-scale performance

Fig. 3 shows the validation results of MOD04_3K highest-quality (QA = 3) AOD retrievals from 2013 to 2017 over the ten regions of interest. The overall accuracy of the aerosol retrievals varies greatly at the continental scale. The AOD retrievals have small estimation uncertainties (e.g., MAE = 0.04–0.06), with ~74–84% of the matchups falling within the EE envelope in Oceania, South Africa, and Eastern North America. Because the surfaces of these regions are relatively dark with dense vegetative cover, surface reflectances are overall low and easily determined, leading to good aerosol estimations.

By contrast, the worse performances are mainly observed in North Africa and the Middle East, Western America, and East Asia. The uncertainties are larger (e.g., MAE > 0.1 and RMSE > 0.15), and only 44–62% of the matchups fall within the EE envelope. These regions are mainly dominated by bright surfaces, with the former two mainly arid or semi-arid regions (e.g., desert, bare land, plateau, or mountain), facing frequent sand/dust and inclement weather conditions (Wei et al., 2018b). East Asia is mainly urban with intensive human activities and a large number of pollution emissions (Nichol and Bilal, 2016; Wei et al., 2019f, g). It is difficult to accurately determine both surface reflectance and aerosol type in these regions, leading to poor aerosol estimations (Li et al., 2009).

In general, except for South Africa (RMB = 1.00), AOD retrievals are overall overestimated in the other regions of interest, especially in Western (RMB = 2.06) and Eastern (RMB = 1.38) North America, and Europe (RMB = 1.46). The inaccuracy of the surface reflectance estimation and the influence of thin cloud contaminations in remote sensing images may explain this (Sun et al., 2016b; Wei et al., 2018b, 2019c). Similar conclusions can be made from the validation results of MOD04_3K all-quality (QA = All) AOD retrievals (Fig. S1). Although the number of effective matchups is reduced, the data quality of AOD retrievals is overall improved, with increasing correlations and percentages of matchups falling within the EE envelope, and decreasing uncertainties after the quality control at the regional scale, especially in Southeast Asia and Eastern America.

3.1.3. Site-scale performance

Analyses on global and regional scales mainly reflect the average overall accuracy of the aerosol product. However, ground stations are not unevenly distributed within a region. Fig. 4 shows the validation of MOD04_3K highest-quality AOD retrievals (QA = 3) against ground measurements from 2013 to 2017 at each AERONET site, revealing the differences at each individual site. There is a total of 10 ground stations with no or too few AOD collocated retrievals, mainly found in North Africa, the Middle East, and Central Australia. Because these stations are located in desert regions, the DT algorithm fails to retrieve AODs over these bright surfaces.

Results suggest heterogeneity of the accuracy of MOD04_3K AODs at the site scale globally. Except for several sites located in the southern parts of South America and Oceania (R < 0.5), AOD retrievals correlate well at most sites, with more than 77% of the sites around the world having R > 0.8 (Fig. 4a). The fraction of retrievals falling within the EE envelope is generally higher than 70% at sites distributed in Europe, Eastern North America, and Central South America. By contrast, it is overall lower than 40% at sites located in the Middle East, Western North America, Southern South America, and East Asia. In general, 69% of the sites globally have more than 60% of the retrievals falling within
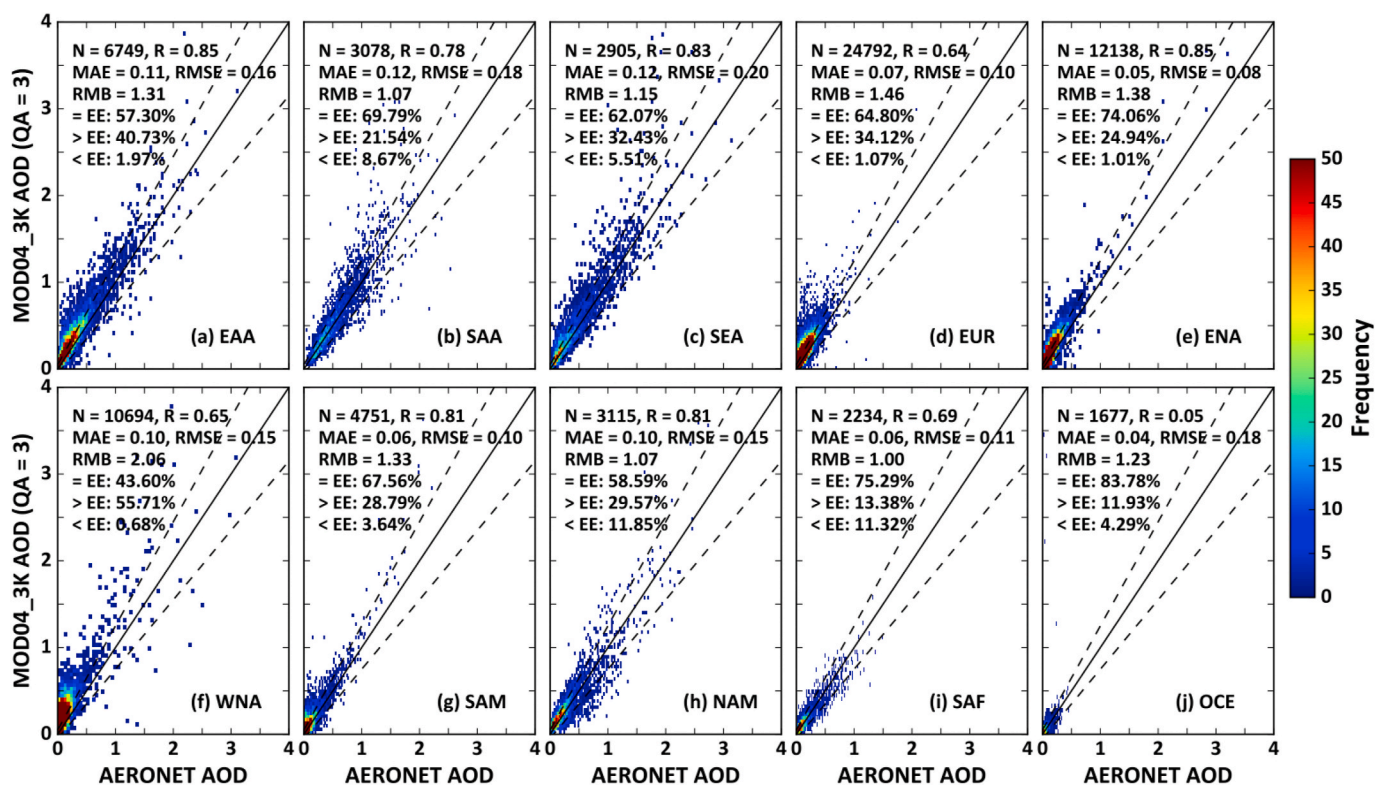
Fig. 3. Same as Fig. 2 but for each region of interest. Only MODIS/Terra 3 km highest-quality (QA = 3) AOD product is used. EAA, SAA, SEA, EUR, ENA, WNA, SAM, NAM, SAF, and OCE stand for East Asia, South Asia, Southeast Asia, Europe, Eastern North America, Western North America, South America, North Africa and the Middle East, South Africa, and Oceania, respectively.
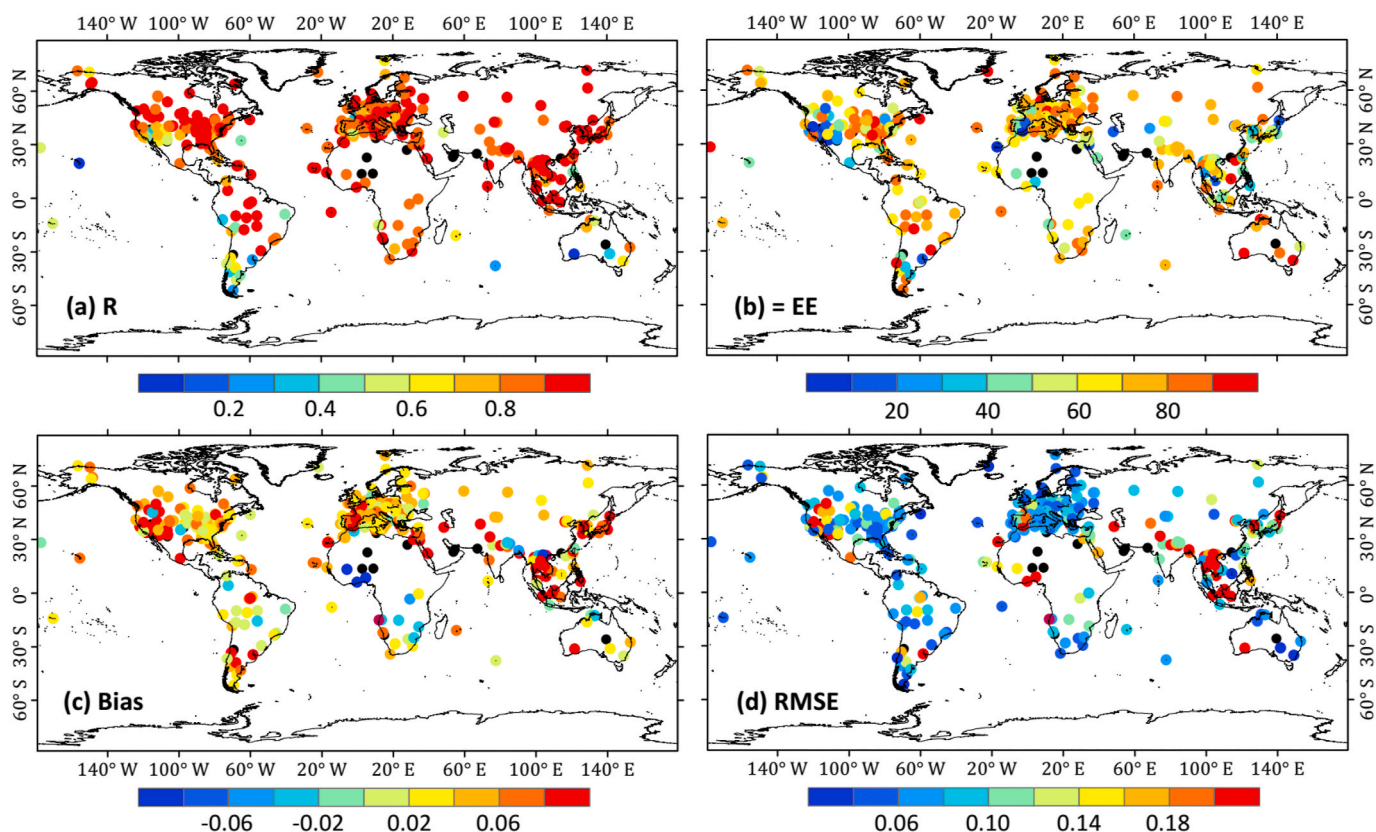
Fig. 4. Validation parameters: (a) correlation coefficient (R), (b) percentage of retrievals falling within the expected error envelope (= EE), (c) mean bias, and (d) root-mean-square error (RMSE) at each AERONET site based on scatter plots of MODIS 3 km AOD retrievals and AERONET AOD measurements from the spatio-temporally collocated data set. Only the MODIS/Terra 3 km highest-quality (QA = 3) AOD product is used. Black dots show those sites with no or too few AOD retrievals.
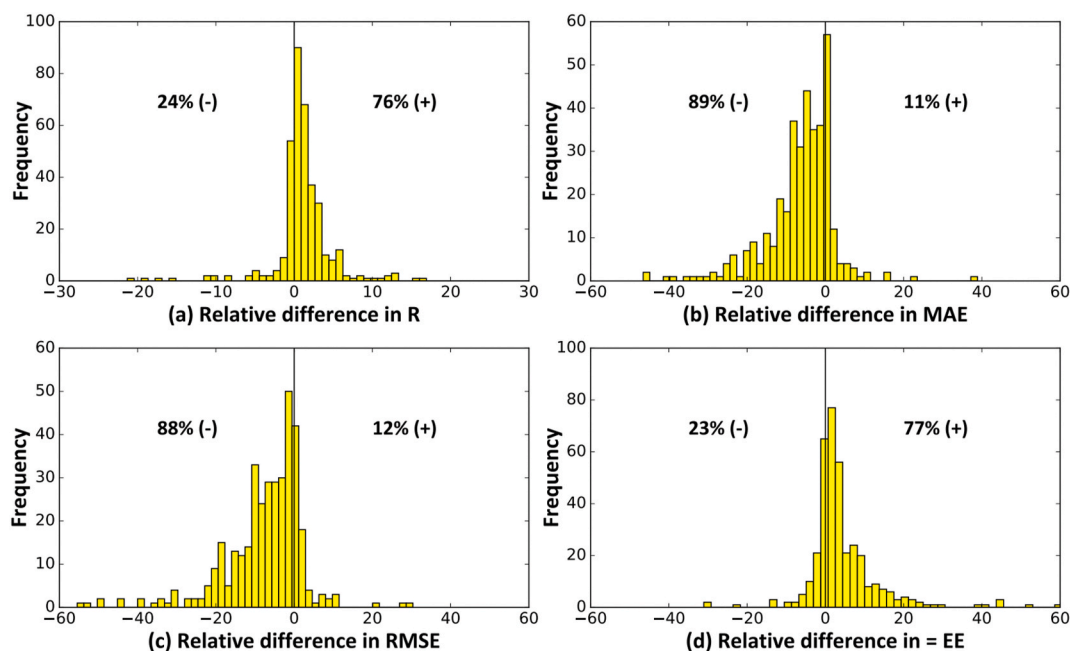

Fig. 5. Frequency histograms of relative differences (%) in validation parameters in terms of (a) correlation coefficient (R), (b) mean absolute error (MAE), (c) root-mean-square error (RMSE), and (d) the percentage of retrievals falling within the expected error envelope (= EE) between MODIS/Terra 3 km highest-quality (QA = 3) and all-quality (QA = All) AOD retrievals for the ensemble of AERONET sites. Annotations in each panel give the proportions of validation statistics, where (+) and (−) indicate positive and negative values.

the EE envelope (Fig. 4b). Only 15% of the sites show small biases within ±0.02. However, ~92% of the sites show positive biases, especially those sites located in the Western North America, Southeast Asia, and East Asia (Fig. 4c). Large negative biases are mainly observed at sites located in Africa and South Asia. This may be related to bright surface structures and strong-absorbing aerosol characteristics (Wei et al., 2018b). In addition, although more than 73% of the sites have small uncertainties with RMSE values < 0.12, large errors (RMSE > 0.2) are always seen at sites located in South and Southeast Asia, Middle Africa, and Western North America, indicating poor estimations (Fig. 4d). The spatial patterns of the four main statistical metrics at the site scale are similar in each season (Figs. S2–S5).

The spatial distributions of the overall accuracies of the MOD04_3K all-quality (QA = All) and MOD04_3K highest-quality (QA = 3) AOD products at the site scale are similar (Fig. S6). However, the four statistical metrics differ. Approximately 75%, 65%, 15%, and 69% of the sites have high correlations (R > 0.8), high percentages of retrievals falling within the EE envelope (> 60%), small biases (~-0.02–0.02), and small uncertainties (RMSE < 0.12), respectively. In general, after data quality control, the accuracy of AOD retrievals is overall improved with increasing correlations, increasing percentages of retrievals falling within the EE envelope, decreasing MAE values, and decreasing RMSE values at ~76%, 77%, 89%, and 88% of the sites, respectively (Fig. 5). However, data quality control does not always perform well, especially when conditions are marginal, which can filter out some normal DT retrievals, especially over bright surfaces (Hubanks and Coauthors, 2013; Wei et al., 2018a).

3.2. Error and uncertainty analysis

The performance of MOD04_3K highest-quality (QA = 3) AOD retrievals under the varying surface and atmospheric aerosol conditions using global AOD matchups (Figs. 6 and 7) are explored here. The surface characterization of each AERONET station is defined as the average value of 5×5 pixels (~225 km^2) of the normalized difference vegetation index (NDVI), surface reflectance, and topography centered on the station. The surface type is defined by the land-use type centered on the AERONET station. The MODIS–AERONET AOD matchups are then filtered by each specific surface and atmospheric aerosol condition and grouped into narrow bins containing different numbers of retrievals in each bin. The number of retrievals, R, mean bias, MAE, RMSE, RMB, and percentages of retrievals falling within/above/below the EE envelope are calculated for each bin (Tables S1–S7).

3.2.1. Relationship with varying surface conditions

The global surface is first divided into 16 NDVI bins with equal bin sizes of 0.05, then MODIS AODs are evaluated against AERONET AODs in each bin (Fig. 6a and Table S1). Overall high accuracy is achieved when NDVI ≤ 0 (e.g., bias = 0.06, fraction = 65%) because this kind of surface mainly includes water bodies without vegetative cover. However, for areas covered by sparse vegetation (0 ≤ NDVI < 0.3), the accuracy is poor, with large positive biases (0.09–0.13) and 37–49% of the retrievals falling within the EE envelope. With an increase in NDVI (0.3 ≤ NDVI < 0.6), the performance improves, characterized by decreasing positive biases and increasing percentages of retrievals falling within the EE envelope. Especially in areas covered by dense vegetation (NDVI ≥ 0.6), the mean bias is < 0.05, and about 67–72% of the retrievals fall within the EE envelope, indicating good data quality.

The global surface is next divided into six main land-use types according to the MODIS land-cover-type product, then MODIS AOD retrievals are validated against ground measurements for each surface type (Fig. 6b and Table S2). Results suggest that the MOD04_3K product performs better, with a smaller bias of 0.05 and RMSE of 0.09 in water (including both inland water and ocean) and forested areas, and more than 69% of the retrievals falling within the EE envelope. This is followed by cropland and grassland, with average biases of 0.07–0.08 and RMSEs of 0.11–0.13. Previous studies have illustrated that the overall accuracy of C6.1 has been improved compared to C6 in urban areas due to the improved surface reflectance model (Gupta et al., 2016). However, AOD retrievals are still overestimated, with a large positive bias of 0.07 and more than 38% of the retrievals falling above the EE envelope. The DT algorithm performs the worst in bare land, with the smallest
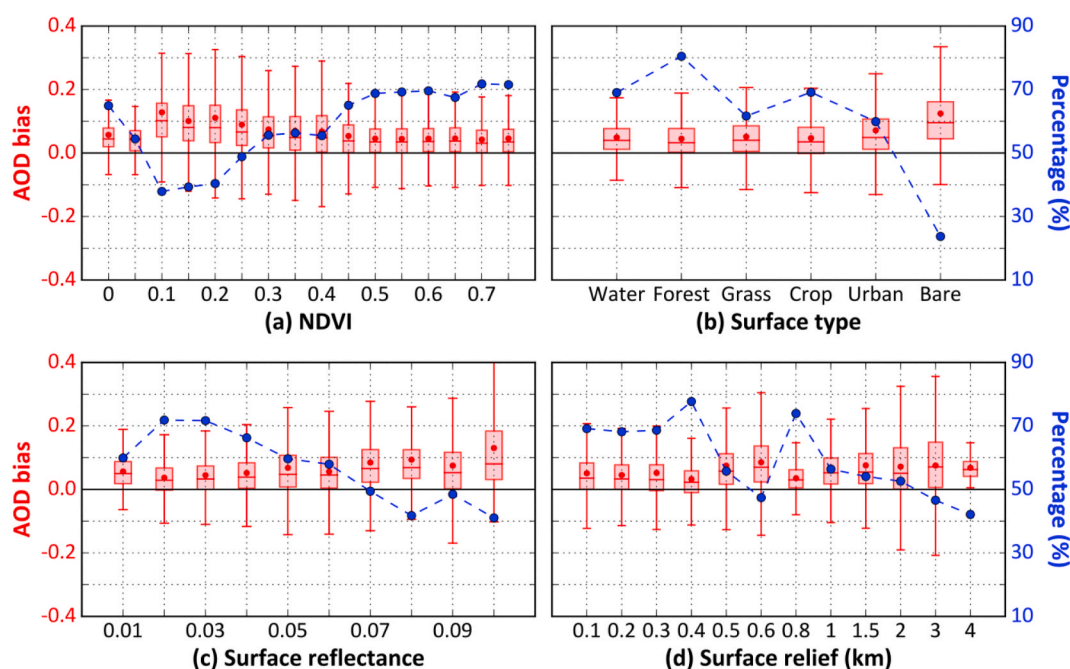

Fig. 6. Box plots of AOD bias (in red) and the percentage of samples falling within the expected error envelope (= EE, blue curves) for MODIS/Terra 3 km highest-quality (QA = 3) AODs against AERONET AODs as a function of (a) NDVI, (b) surface type, (c) surface reflectance (459–479 nm), and (d) surface relief (km). The black horizontal solid line represents the zero bias. In each box, the red dots, middle, lower, and upper horizontal lines represent the AOD bias mean, median, and 25th and 75th percentiles, respectively. (For interpretation of the references to color in this figure legend, the reader is referred to the Web version of this article.)
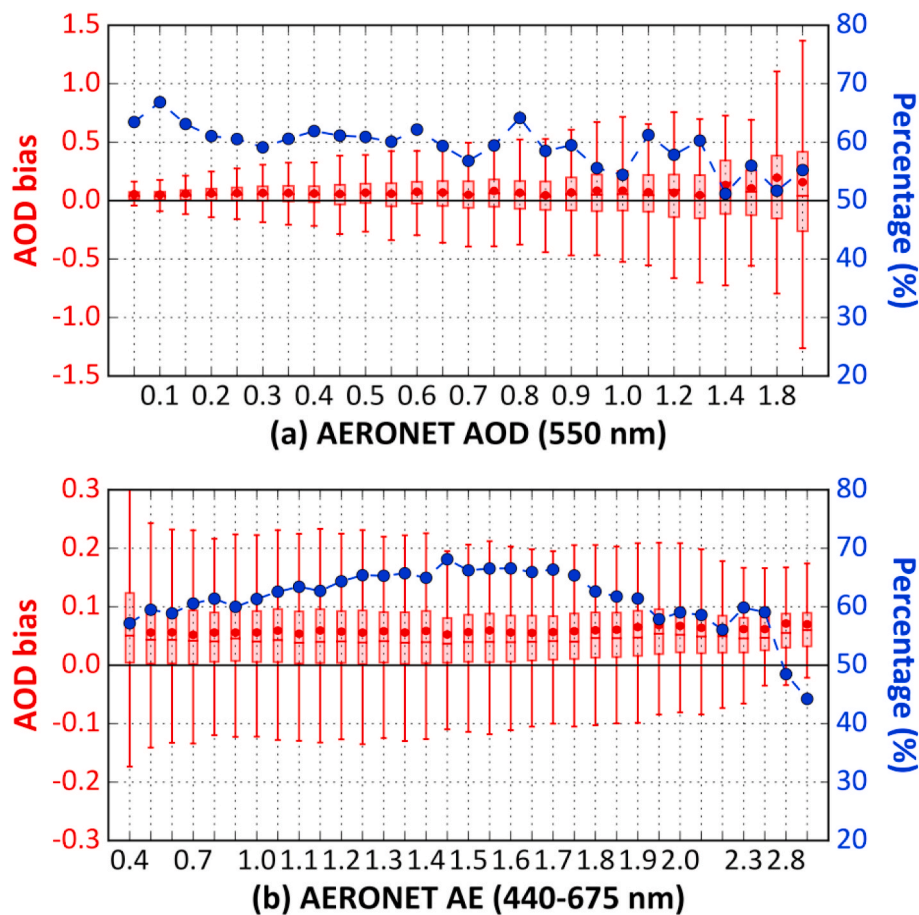
Fig. 7. Same as Fig. 6 but for varying atmospheric aerosol conditions as a function of AERONET (a) AOD (550 nm) and (b) AE (440–675 nm) measurements.

number of matchups (N = 1287) and the worst evaluation metrics, in particular, only 39% of the retrievals falling within the EE envelope. These results suggest that the DT algorithm still faces great challenges in retrieving aerosol properties over heterogeneous urban and bright bare surfaces.

Next, the global land surface is divided into ten MODIS surface reflectance (459–479 nm) bins with equal bin sizes of 0.01, and MODIS AOD retrievals are assessed with surface measurements from darkest to brightest surfaces (Fig. 6c and Table S3). The DT algorithm performs better when the surface is darker (land surface reflectance, or LSR < 0.04), such as water, dark soil, and dense vegetation, with small uncertainties (e.g., bias < 0.06, RMSE < 0.12) and more than 60% of the matchups falling within the EE envelope. However, as the surface becomes brighter, the overall accuracy of the aerosol retrievals decreases rapidly, and the estimation uncertainty increases significantly. Especially for brighter surfaces (LSR > 0.08) such as deserts, bare land, and urban buildings, the retrievals have larger positive uncertainties (e.g., bias > 0.08, RMSE > 0.24) and smaller percentages falling within the EE envelope (41–49%). The main reason is that the surface reflectance relationships between visible and shortwave-infrared channels become increasingly unstable and difficult to determine accurately, leading to poor aerosol retrievals (Wei et al., 2018a, b).

Finally, the global land surface is divided into 13 surface relief bins with different bin sizes, calculated from the Shuttle Radar Topography Mission (SRTM) digital elevation model (DEM) product. Surface relief refers to the degree of altitude changes and topographic fluctuations of a land area, calculated as the difference between the maximum elevation and the minimum elevation in a sliding window (Wei et al., 2019d). MODIS AOD retrievals are then validated against surface observations with changes in topography (Fig. 6d and Table S4). The overall accuracy

of the retrievals is relatively high, with relatively small estimation biases (< 0.05) and more than 68% of the matchups falling within the EE envelope in areas with small surface fluctuations (surface relief < 0.4 km), such as plains, basins, and hills. However, with increasing surface relief, the data quality of aerosol retrievals gradually deteriorates, with increasing estimation biases and uncertainties. In particular, for steep mountainous and plateau areas (surface relief > 2 km), the DT algorithm performance worsens, with a larger positive estimation bias and less than 47% of the matchups falling within the EE envelope. This is because the DT algorithm does not take the impact of terrain or mountain artifacts into account (Wei et al., 2019c, d).

3.2.2. Relationship with varying atmospheric aerosol conditions

The atmospheric aerosol conditions are divided into 27 AERONET AOD (550 nm) bins, 33 AE (440–675 nm) bins and 21 SSA (550 nm) bins with different bin sizes. Note that the number of retrievals in each bin is different, with many lower AOD values in the mid-range of AE values. The AOD retrievals are then evaluated (Figs. 7 and 8). Tables S5–S7 summarize the number of retrievals and the statistical results for each bin.

Under low aerosol loading conditions (AOD < 0.3), the retrievals show good overall accuracy (Fig. 7a), and the estimation uncertainties are relatively small (e.g., MAE < 0.1, RMSE < 0.13), although there is overestimation (RMB > 1.2). However, as the aerosol loading increases (0.3 ≤ AOD < 1.0), the retrieval uncertainty increases, and the percentage of retrievals falling within the EE envelope decreases gradually, as does the overestimation. In particular, there are large retrieval errors under high aerosol loading conditions (AOD ≥ 1.0). This is because the sources and compositions of aerosols are complex and difficult to determine when the aerosol loading is high, making aerosol retrievals
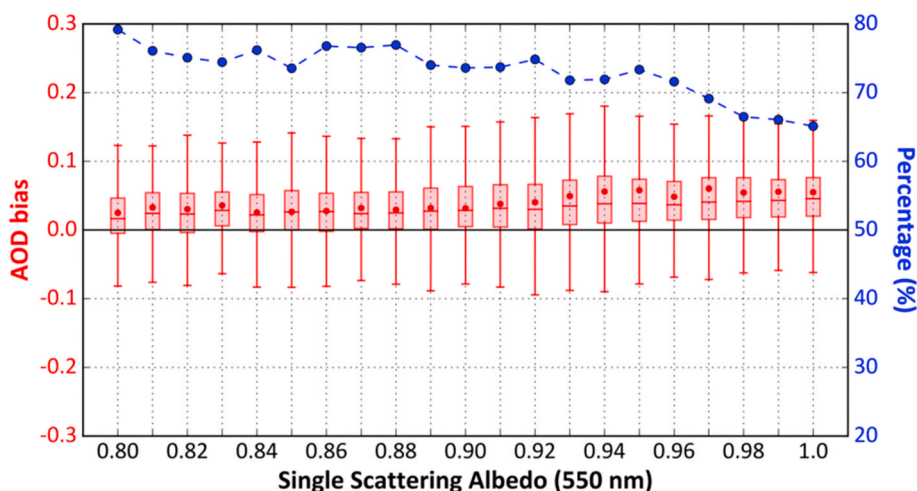
Fig. 8. Same as Fig. 6 but as a function of AERONET single scattering albedo (SSA, 550 nm) measurements.

less accurate.

For large-sized aerosol particles (AE < 0.8) mainly dominated by coarse mineral dust, AOD retrievals have overall large uncertainties (e. g., MAE > 0.08, RMSE > 0.13), with less than 60% of the retrievals falling within the EE envelope (Fig. 7b). For medium-sized aerosol particles (0.8 ≤ AE < 1.4) that are mixtures of fine- and coarse-mode particles, the overall accuracy is gradually improved, with more stable biases and increasing percentages of retrievals falling within the EE envelope as AE increases. However, for small-sized aerosol particles (1.4 ≤ AE < 2.5), the performance of the DT algorithm gradually worsens, with increasing positive biases and decreasing percentages of retrievals falling within the EE envelope as AE increases. In particular, for finer-mode aerosol particles (AE ≥ 2.5), AOD retrievals are highly uncertain with larger positive biases (> 0.07) and with greater than 51% of the retrievals falling above the EE envelope, indicating large overestimations (i.e., RMB > 3.5).

AOD retrievals for five main aerosol types diagnosed by the MODIS 3 km algorithm are evaluated next. These are used to inform developers and users about which processing path was followed during processing (https://darktarget.gsfc.nasa.gov/atbd/land-algorithm). Here, only collocated AOD matchups over land are used and sorted for each diagnostic aerosol type (Table 2). For areas with weakly absorbing aerosols, AOD retrievals have the best accuracy, with the smallest MAE of 0.06 and RMSE of 0.08, and with more than 72% of the retrievals falling within the EE envelope. By contrast, for areas diagnosed with continental and dust aerosols, the number of data samples is smaller, and AOD retrievals have larger estimation errors, with 52–69% of the retrievals falling above the EE envelope. The statistics for areas diagnosed with strongly and moderately absorbing aerosols fall somewhere in between. These results suggest again that the sources and compositions of aerosols are complex and vary spatiotemporally over land. However, these diagnostic aerosol types are mainly defined by region, and their optical characteristics are fixed. More representative and appropriate is a less restrictive set of aerosol-type models, which has been proved to improve the overall accuracy of retrievals, especially in local regions (e. g., Eastern China) with complex and variable aerosol components (Wei

et al., 2017, 2019f, g).

Furthermore, the uncertainty of DT AOD retrievals related to the true aerosol type is also evaluated according to the AERONET SSA measurements (Fig. 8). For strong absorbing aerosol conditions (SSA < 0.88), e.g., urban or industrial regions, the retrievals show small estimation uncertainties (e.g., MAE = 0.05, RMSE = 0.07) with an average bias of 0.03, and approximately 76% of the data samples falling within the EE envelope, suggesting good data quality (Table S7). When the aerosols gradually become less absorbing (0.88 ≤ SSA < 0.95), e.g., developing world, the accuracy of retrievals gradually declined with increasing positive biases and RMSE values, and decreasing fractions falling within the EE envelope. However, for week absorbing or spheroid aerosol conditions (SSA ≥ 0.95), e.g., smoke and dust, the retrievals become increasingly unreliable with large estimation uncertainties, and only approximately 68% of them falling within the EE envelope, showing large overestimations (RMB = 1.48). In general, the results here are similar to those concluded from the above diagnostic certain aerosol types.

3.3. Comparison with MOD04_L2 products

In this section, MOD04_3K highest-quality (QA = 3) AOD retrievals (3 km) are compared with MOD04_L2 highest-quality (QA = 3) AOD retrievals (10 km) at different spatial scales from 2013 to 2017. Fig. 9 shows the relative differences (%) in four main statistical metrics (i.e., MAE, RMSE, RMB, and percentage of matchups falling within the EE envelope) between MODIS 3 km and 10 km AOD products in each region of interest. In general, there are clear differences in the performance between these two aerosol products on a regional scale. Similar performances with relatively small differences in all evaluation indicators are observed for SAA, SAF, and SEA. By contrast, MOD04_3K AOD products are less accurate than MOD04_L2 AOD products in the remaining regions, especially North America and Oceania, with increasing MAE, RMSE, and RMB values by 4–30%, 3–64%, and 5–22%, respectively, and decreasing percentages of matchups falling within the EE envelope (6–34%).

Table 2

Statistics of the accuracy and uncertainty of AOD retrievals for different diagnostic aerosol types over land.

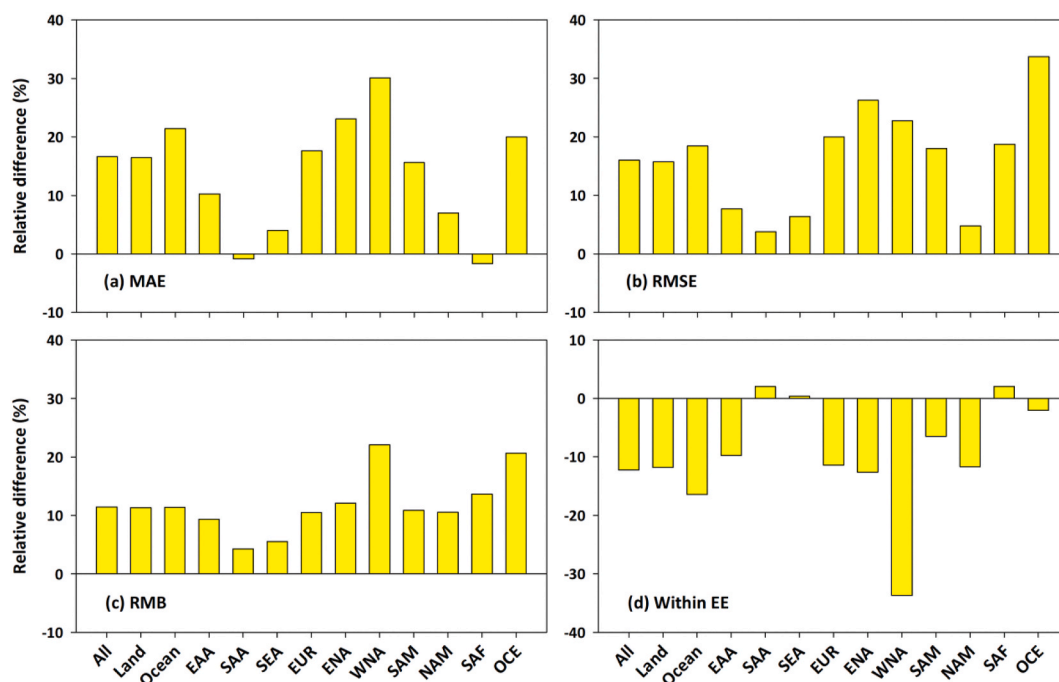| Aerosol type	N	R	Bias	MAE	RMSE	RMB	= EE	> EE	< EE
Continental	1157	0.91	0.08	0.10	0.14	1.41	43.65	52.72	3.63
Moderate absorption	48,862	0.88	0.06	0.08	0.13	1.36	60.98	36.15	2.88
Strong absorption	3954	0.91	0.07	0.13	0.20	1.14	64.26	29.49	6.25
Weak absorbtion	13,380	0.90	0.04	0.06	0.08	1.34	72.04	26.89	1.07
Dust	247	0.67	0.11	0.12	0.25	1.73	30.77	68.83	0.40

Fig. 9. Relative differences (%) in terms of validation parameters: (a) mean absolute error (MAE), (b) root-mean-square error (RMSE), (c) relative mean bias (RMB), and (d) percentage of retrievals falling within the expected error (EE) envelope between MODIS/Terra 3 km and 10 km highest-quality (QA = 3) AOD products for each region of interest. The black horizontal solid line represents the zero bias. EAA, SAA, SEA, EUR, ENA, WNA, SAM, NAM, SAF, and OCE stand for East Asia, South Asia, Southeast Asia, Europe, Eastern North America, Western North America, South America, North Africa and the Middle East, South Africa, and Oceania, respectively.
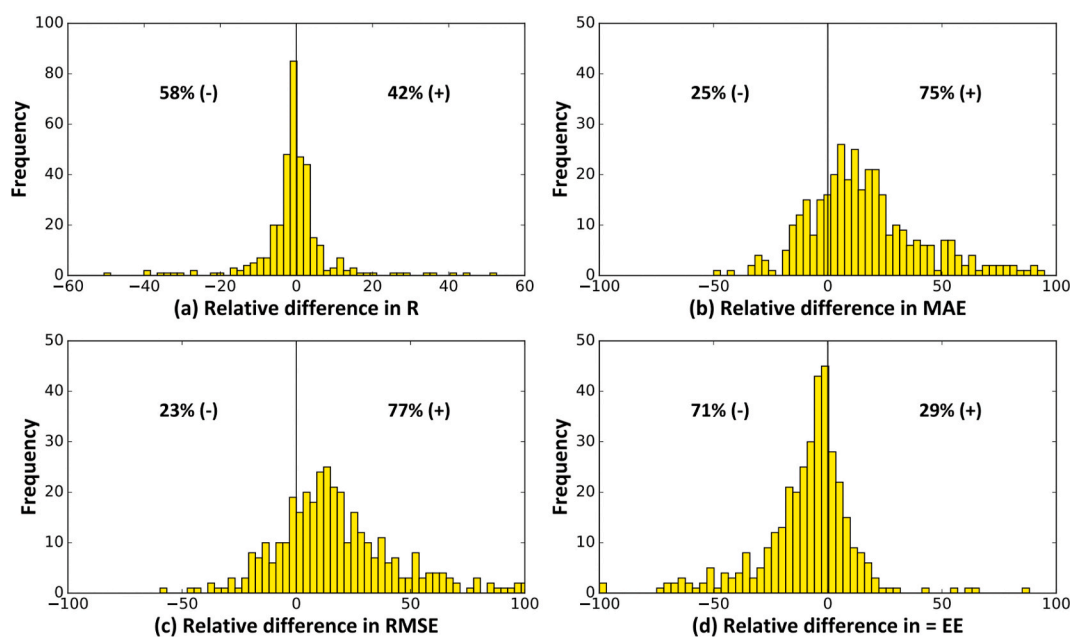

Fig. 10. Frequency histograms of relative differences (%) in terms of (a) correlation coefficient (R), (b) mean absolute error (MAE), (c) root-mean-square error (RMSE), and (d) the percentage of retrievals falling within the expected error (EE) envelope between Terra MODIS 3 km and 10 km highest-quality (QA = 3) AOD retrievals for the ensemble of sites. Annotations in each panel give the proportions of validation statistics, where (+) and (−) indicate positive and negative values.

Fig. 10 shows the frequency histograms of differences in four main statistical metrics between MOD04_3K (3 km) and MOD04_L2 (10 km) highest-quality (QA = 3) AOD retrievals for the ensemble of sites. At the site scale, with reference to 10 km AOD retrievals, MODIS 3 km AOD retrievals have decreasing R values in ~58% of the sites around the world. However, MAE and RMSE values increase at 75% and 77% of the global sites, respectively. More importantly, ~71% of the sites have decreasing percentages of matchups falling within the EE envelope. In general, the data quality of the MOD04_3K AOD product is lower than that of the MOD04_L2 AOD product at global to regional to site scales.
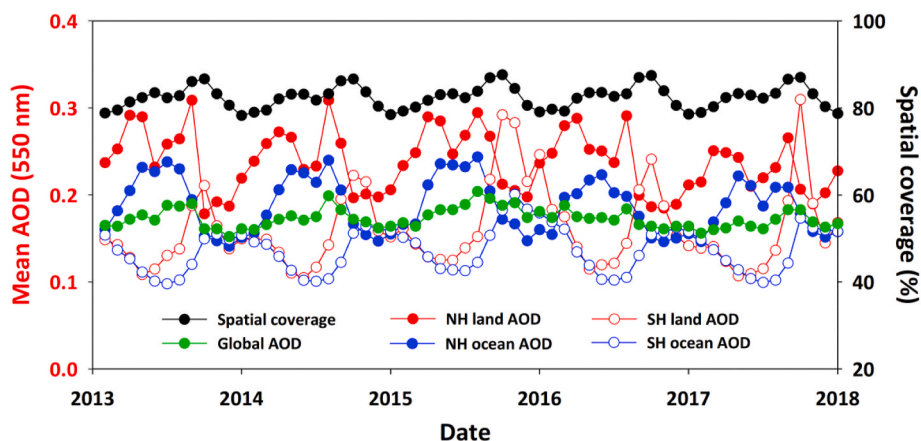
Fig. 11. Time series of monthly global spatial coverage (in black) and monthly mean AODs over the globe (in green), land (in red), and ocean (in blue) in the Northern Hemisphere (NH) and Southern Hemisphere (SH) from 2013 to 2017. (For interpretation of the references to color in this figure legend, the reader is referred to the Web version of this article.)

The main reason for the degradation of the retrieval accuracy of the finer-resolution product is a decrease in opportunity to discard marginal pixels from the retrieval (Remer et al., 2013) or the increase of image signal-to-noise ratio (Wei and Sun, 2017).

3.4. Spatiotemporal coverage and distribution

In this section, the ability of the MODIS DT aerosol algorithm to describe the spatiotemporal aerosol variations from global to regional scales is investigated. For this purpose, the MODIS Level 3 atmospheric global monthly gridded product ($1° \times 1°$), aggregated from the more accurate MOD04 10 km aerosol product based on the same DT algorithm (Platnick et al., 2015), is selected for analysis. Fig. 11 shows the time series of monthly satellite observations in terms of spatial coverage and mean AOD from 2013 to 2017 over the globe, land, and oceans, respectively. The spatial coverage varies interannually, with a wider spatial coverage seen in August and September, reaching 86–88%. In December and January, due to permanent snow/ice cover at the high latitudes of the Northern Hemisphere, there are more missing values, with an average narrower spatial coverage of 78–80% (Fig. 12d).

Regarding aerosol loadings, although there are some differences over time, the global average AOD generally remains stable, ranging from 0.15 to 0.20 with a small standard deviation of 0.01. By contrast, there are clear differences in mean AOD loadings over land and oceans. The aerosol loading over land is much higher than over ocean, especially in the Northern Hemisphere (average = 0.24 versus 0.19). In addition,
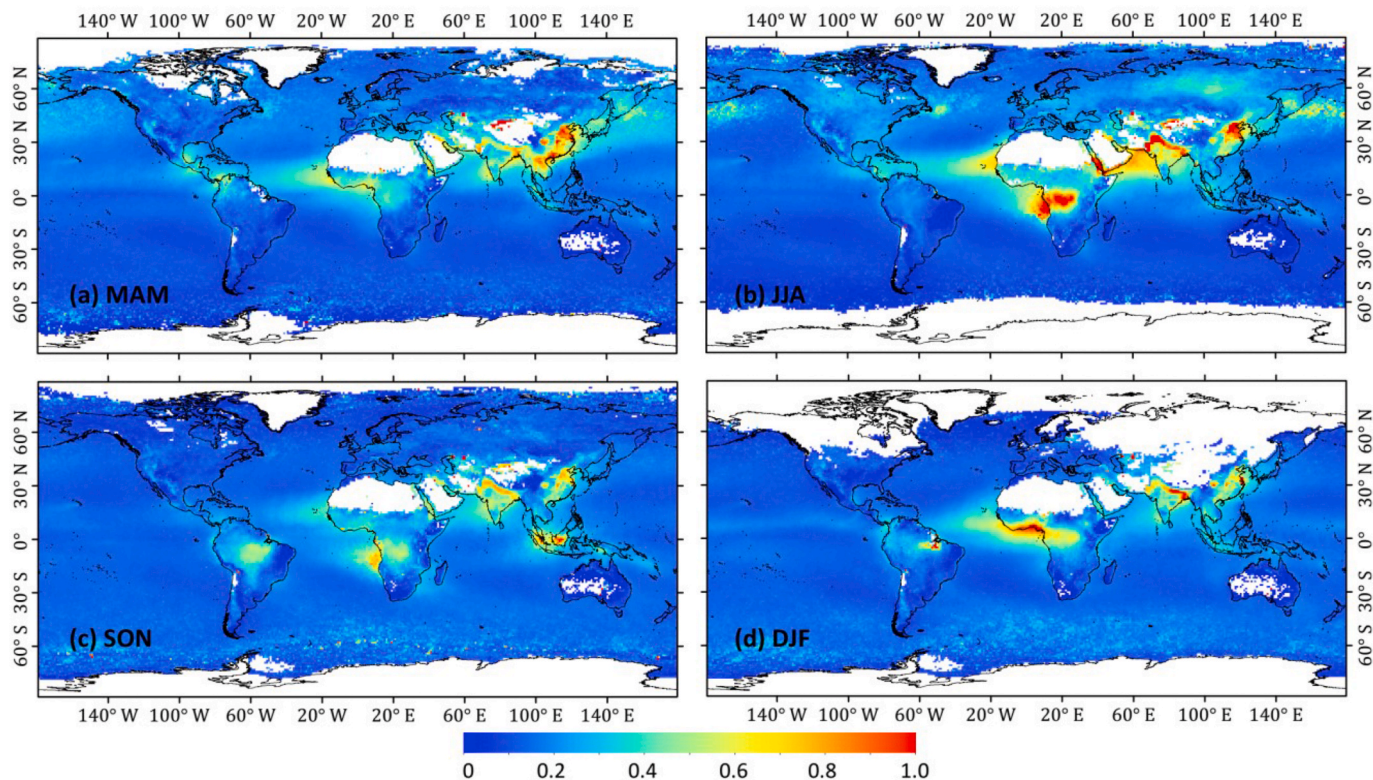

Fig. 12. Spatial distributions of seasonal mean AODs (550 nm) in (a) March-April-May (MAM), (b), June-July-August (JJA), (c) September-October-November (SON), and (d) December-January-February (DJF) from 2013 to 2017.

Table 3

Statistics of seasonal and annual mean AODs over the world and for each region of interest from 2013 to 2017. EAA, SAA, SEA, EUR, ENA, WNA, SAM, SAF, and OCE stand for East Asia, South Asia, Southeast Asia, Europe, Eastern North America, Western North America, South America, South Africa, and Oceania, respectively.

Region	MAM	JJA	SON	DJF	Annual
Global	0.17 ± 0.11	0.18 ± 0.14	0.16 ± 0.10	0.17 ± 0.10	0.17 ± 0.10
Land	0.21 ± 0.17	0.24 ± 0.18	0.18 ± 0.16	0.20 ± 0.15	0.20 ± 0.15
Ocean	0.16 ± 0.09	0.16 ± 0.11	0.16 ± 0.08	0.16 ± 0.08	0.16 ± 0.07
EAA	0.25 ± 0.21	0.27 ± 0.15	0.18 ± 0.13	0.27 ± 0.18	0.22 ± 0.14
SAA	0.44 ± 0.16	0.56 ± 0.29	0.45 ± 0.28	0.47 ± 0.22	0.47 ± 0.28
SEA	0.36 ± 0.22	0.25 ± 0.08	0.37 ± 0.20	0.26 ± 0.09	0.31 ± 0.09
EUR	0.18 ± 0.16	0.22 ± 0.17	0.16 ± 0.16	0.15 ± 0.15	0.18 ± 0.15
ENA	0.17 ± 0.06	0.20 ± 0.06	0.11 ± 0.03	0.10 ± 0.04	0.15 ± 0.05
WNA	0.16 ± 0.06	0.20 ± 0.06	0.10 ± 0.04	0.11 ± 0.05	0.15 ± 0.04
SAM	0.14 ± 0.09	0.12 ± 0.08	0.21 ± 0.13	0.18 ± 0.14	0.16 ± 0.08
SAF	0.14 ± 0.10	0.27 ± 0.29	0.24 ± 0.15	0.19 ± 0.14	0.21 ± 0.16
OCE	0.07 ± 0.13	0.06 ± 0.13	0.10 ± 0.18	0.09 ± 0.11	0.07 ± 0.13

aerosol loadings vary seasonally with large fluctuations globally (i.e., standard deviation ranging from 0.03 to 0.05), especially over land. In general, high aerosol loadings are often observed around June and July, and low aerosol loadings are always found around October and November in the Northern Hemisphere. The opposite is seen in the Southern Hemisphere due to the reversed seasons between the two hemispheres.

Fig. 12 shows the global spatial distributions of AOD loadings in different seasons from 2013 to 2017. Table 3 summarizes the statistical results. The seasonal AOD maps cover almost all oceans and most land surfaces with an average spatial coverage of 90% (March-April-May, MAM), 90% (June-July-August, JJA), 92% (September-October-November, SON), and 84% (December-January-February, DJF). In general, except for some coastal areas (e.g., the west coast of Africa, inshore areas of India and East Asia), seasonal mean AODs are generally low with an average of 0.16, especially over open seas far away from the influence of human activities. However, aerosol loadings are spatially and temporally heterogeneous over land. Again, the DT algorithm cannot make retrievals over bright surfaces, so there are numerous missing values seen in North Africa, the Middle East, Central Asia, and central Australia, where deserts dominate.

In general, high aerosol loadings are observed over India, East Asia, central Africa, and Southeast Asia due to the large amounts of anthropogenic aerosols emitted into the air from intensive human activities. By contrast, aerosol loadings are generally low over most of the remaining regions of interest, especially Europe, North America, and Oceania. In June, July, and August (JJA), air pollution is the most severe with the highest mean aerosol loading of 0.24 ± 0.18, especially in South Asia (0.56 ± 0.29), South Africa (0.27 ± 0.29), and East Asia (0.27 ± 0.15). The smallest mean AOD values are found over most land surfaces in September, October, and November (SON). In the other seasons, aerosol loadings over most continents are similar.

4. Conclusions and discussion

In this study, an initial overview and validation of the latest Terra MODIS Collection 6.1 daily aerosol product at a higher spatial resolution of 3 km is performed. For this purpose, the MODIS 3 km DT global daily AOD product (MOD04_3K) from 2013 to 2017 is validated against the newest AERONET Version 3 AOD measurements at 384 monitoring sites distributed across land and ocean. The validation is performed at global to continental to site scales, and the errors and uncertainties related to varying surface and atmospheric aerosol characteristics are discussed. The spatiotemporal characteristics and variations are also investigated. Results obtained in this study provide a clearer and better understanding of the global MOD04_3K aerosol product.

Although the MOD04_3K AOD product performs well on a global scale, there are noticeable differences in the accuracy and the uncertainty at regional to site scales. The worst performance is mainly observed in North Africa and the Middle East, Western North America,

and East Asia. More importantly, AOD retrievals are overall overestimated with positive biases at more than 92% of the sites around the world. In general, the data quality of the aerosol product is overall improved at all spatial scales after data quality control. The error and uncertainty analyses illustrate that with increasing surface reflectance and surface relief, the bias of AOD estimates increases. The DT algorithm performs less well when the aerosol loading is high with large Ångström exponents, suggesting a poorer performance when fine particles dominate. Note that this scenario represents only 15% of the total database. With reference to the 10 km AOD retrievals, the 3 km AOD retrievals have larger estimation uncertainties caused mainly by a decrease in the opportunity to discard marginal pixels from the retrieval. Monthly MODIS AOD maps cover ~78–88% of the globe and can describe well the spatiotemporal characteristics of global AOD loadings except over bright surfaces in North Africa, the Middle East, and central Asia.

In general, compared to the previous validation work done on the C6 3 km aerosol product (Gupta et al., 2018), results here suggest that the accuracy of the C6.1 3 km aerosol product has been overall improved. Although some similar conclusions can be obtained here in terms of the overall accuracy changes with spatial scale, quality assurance, spatial resolution, and aerosol loading, mainly because some small changes were made to the C6 and C6.1 3 km retrieval algorithms, this study provides additional valuable information by extending the evaluation to coastal waters in offshore seas where the C6.1 DT algorithm mainly updates, and by carrying out an in-depth uncertainty analysis involving varying surface characteristics. Future work will evaluate AOD retrievals from currently available MODIS or other satellite aerosol products generated from different algorithms over open seas away from the shoreline using measurements from the Maritime Aerosol Network (MAN). A focus will also be placed on improving the aerosol retrieval algorithm so that the overall estimation uncertainty is reduced, and the spatial resolution is improved, of great importance to related air pollution studies at medium to small scales, e.g., at the urban scale.

Appendix A. Supplementary data

Supplementary data to this article can be found online at https://doi.org/10.1016/j.atmosenv.2020.117768.

References

Bartell, S.M., Longhurst, J., Tjoa, T., Sioutas, C., Delfino, R.J., 2013. Particulate air pollution, ambulatory heart rate variability, and cardiac arrhythmia in retirement community residents with coronary artery disease. Environ. Health Perspect. 121 (10), 1135–1141. https://doi.org/10.1289/ehp.1205914.

Bright, J., Gueymard, C., 2019. Climate-specific and global validation of MODIS Aqua and Terra aerosol optical depth at 452 AERONET stations. Sol. Energy 183, 594–605. https://doi.org/10.1016/j.solener.2019.03.043.

Charlson, R.J., Schwartz, S.E., Hales, J.M., Cess, R.D., Coakley, J.A., Hansen, J.E., Hoffman, D.J., 1992. Climate forcing by anthropogenic aerosols. Science 255 (5043), 423–430. https://doi.org/10.1126/science.255.5043.423.

Fan, A., Chen, W., Liang, L., Sun, W., Lin, Y., Che, H., Tao, X., 2017. Evaluation and comparison of long-term MODIS C5.1 and C6 products against AERONET observations over China. Rem. Sens. 9, 1269. https://doi.org/10.3390/rs9121269.

Giles, D.M., Sinyuk, A., Sorokin, M.S., Schafer, J.S., Smirnov, A., Slutsker, I., Eck, T.F., Holben, B.N., Lewis, J.R., Campbell, J.R., Welton, E.J., Korkin, S., Lyapustin, A., 2019. Advancements in the Aerosol Robotic Network (AERONET) Version 3 database - automated near real-time quality control algorithm with improved cloud screening for Sun photometer aerosol optical depth measurements. Atmos. Meas. Tech. 12, 169–209. https://doi.org/10.5194/amt-12-169-2019.

Gupta, P., Levy, R.C., Mattoo, S., Remer, L.A., Munchak, L.A., 2016. A surface reflectance scheme for retrieving aerosol optical depth over urban surfaces in MODIS Dark Target retrieval algorithm. Atmos. Meas. Tech. 9, 3293–3308. https://doi.org/10.5194/amt-9-3293-2016.

Gupta, P., Remer, L.A., Levy, R.C., Mattoo, S., 2018. Validation of MODIS 3 km land aerosol optical depth from NASA's EOS Terra and Aqua missions. Atmos. Meas. Tech. 11, 3145–3159. https://doi.org/10.5194/amt-11-3145-2018.

Haywood, J., Boucher, O., 2000. Estimates of the direct and indirect radiative forcing due to tropospheric aerosols: a review. Rev. Geophys. 38 (4), 513–543. https://doi.org/10.1029/1999RG000078.

He, Q., Zhang, M., Huang, B., Tong, X., 2017. MODIS 3 km and 10 km aerosol optical depth for China: evaluation and comparison. Atmos. Environ. 153, 150–162. https://doi.org/10.1016/j.atmosenv.2017.01.023.

Holben, B.N., Eck, T.F., Slutsker, I., Tanre, D., Buis, J.P., Setzer, A., Vermote, E., Reagan, J.A., Kaufman, Y.J., Nakajima, T., Lavenu, F., Jankowiak, I., Smirnov, A., 1998. Aeronet – a federated instrument network and data archive for aerosol characterization. Rem. Sens. Environ. 66, 1–16. https://doi.org/10.1016/S0034-4257(98)00031-5.

Hubanks, P., Coauthors, 2013. MODIS Atmosphere QA Plan for Collection 005 and 051 (Includes Cirrus Flag & High Cloud Flag (06_CT) Clarification, Deep Blue Aerosol Update, Aerosol over Land Update, Water Vapor and Atmosphere Profile Update, Changes to MOD35 QA Bit Field Documentation) Version 3.10.

Jeong, M.-J., Hsu, N.C., Kwiatkowska, E.J., Franz, B.A., Meister, G., Salustro, C.E., 2011. Impacts of cross-platform vicarious calibration on the Deep Blue aerosol retrievals for moderate resolution imaging spectroradiometer aboard Terra. IEEE Trans. Geosci. Rem. Sens. 49 (12), 4877–4988. https://doi.org/10.1109/TGRS.2011.2153205.

Kaufman, Y.J., Tanré, D., Remer, L., Vermote, E., Chu, A., Holben, B.N., 1997. Operational remote sensing of tropospheric aerosol over land from EOS moderate resolution imaging spectroradiometer. J. Geophys. Res. Atmos. 102, 17. https://doi.org/10.1029/96JD03988, 051–17,067.

Koren, I., Altaratz, O., Remer, L.A., Feingold, G., Martins, J.V., Heiblum, R.H., 2012. Aerosol-induced intensification of rain from the tropics to the mid-latitudes. Nat. Geosci. 5, 118–122. https://doi.org/10.1038/ngeo1364.

Levy, R.C., Mattoo, S., Munchak, L.A., Remer, L.A., Sayer, A.M., Patadia, F., Hsu, N.C., 2013. The Collection 6 MODIS aerosol products over land and ocean. Atmos. Meas. Tech. 6, 2989–3034. https://doi.org/10.5194/amt-6-2989-2013.

Levy, R.C., Remer, L.A., Kleidman, R.G., Mattoo, S., Ichoku, C., Kahn, R., Eck, T.F., 2010. Global evaluation of the Collection 5 MODIS dark-target aerosol products over land. Atmos. Chem. Phys. 10 (10) https://doi.org/10.5194/acp-10-10399-2010, 399–10,420.

Li, Z., Zhao, X., Kahn, R., Mishchenko, M., Remer, L., Lee, K.-H., Wang, M., Laszlo, I., Nakajima, T., Maring, H., 2009. Uncertainties in satellite remote sensing of aerosols and impact on monitoring its long-term trend: a review and perspective. Ann. Geophys. 27, 1–16. https://doi.org/10.5194/angeo-27-2755-2009.

Li, Z., Rosenfeld, D., Fan, J., 2017. Aerosols and Their Impact on Radiation, Clouds, Precipitation, and Severe Weather Events. Oxford Research Encyclopedias. https://doi.org/10.1093/acrefore/9780199389414.013.126.

Li, Z., Coauthors, 2017. Aerosols and boundary-layer interactions and impact on air quality. Natl. Sci. Rev. 4, 810–833. https://doi.org/10.1093/nsr/nwx117.

Ma, Q., Li, Y., Liu, J., Chen, J., 2017. Long temporal analysis of 3-km MODIS aerosol product over East China. IEEE J. Select. Top. Appl. Earth Obs. Rem. Sens. 10 (6), 2478–2490. https://doi.org/10.1109/JSTARS.2017.2650144.

Meister, G., Eplee, R.E., Franz, B.A., 2014. Corrections to MODIS Terra calibration and polarization trending derived from ocean color products. In: Proc. SPIE 9218, Earth Observing Systems XIX, p. 9218V. https://doi.org/10.1117/12.2062714.

Munchak, L.A., Levy, R.C., Mattoo, S., Remer, L.A., Holben, B.N., Schafer, J.S., Hostetler, C.A., Ferrare, R.A., 2013. MODIS 3 km aerosol product: applications over land in an urban/suburban region. Atmos. Meas. Tech. 6, 1747–1759. https://doi.org/10.5194/amt-6-1747-2013.

Nichol, J., Bilal, M., 2016. Validation of MODIS 3 km resolution aerosol optical depth retrievals over Asia. Rem. Sens. 8, 328. https://doi.org/10.3390/rs8040328.

Oreopoulos, L., Cho, N., Lee, D., Kato, S., 2016. Radiative effects of global MODIS cloud regimes. J. Geophys. Res. Atmos. 121, 2299–2317. https://doi.org/10.1002/2015JD024502.

Peng, R.D., Bell, M.L., Geyh, A.S., McDermott, A., Zeger, S.L., Samet, J.M., Dominici, F., 2009. Emergency admissions for cardiovascular and respiratory diseases and the chemical composition of fine particle air pollution. Environ. Health Perspect. 117 (6), 957–963. https://doi.org/10.1289/ehp.0800185.

Platnick, S., Hubanks, P., Meyer, K., King, M.D., 2015. MODIS Atmosphere L3 Monthly Product (08_L3). NASA MODIS Adaptive Processing System. Goddard Space Flight Center. https://doi.org/10.5067/MODIS/MOD08_M3.006.

Qin, W., Wang, L., Wei, J., Hu, B., Liang, X., 2020. A novel efficient broadband model to derive daily surface solar Ultraviolet radiation (0.280-0.400 μm). Sci. Total Environ. 735, 139153. https://doi.org/10.1016/j.scitotenv.2020.139153.

Remer, L., Mattoo, S., Levy, R., Munchak, L., 2013. MODIS 3 km aerosol product: algorithm and global perspective. Atmos. Meas. Tech. 6, 1829–1844. https://doi.org/10.5194/amt-6-1829-2013.

Sayer, A.M., Govaerts, Y., Kolmonen, P., Lipponen, A., Luffarelli, M., Mielonen, T., Patadia, F., Popp, T., Povey, A.C., Stebel, K., Witek, M.L., 2019. A review and framework for the evaluation of pixel-level uncertainty estimates in satellite aerosol remote sensing. Atmos. Meas. Tech. https://doi.org/10.5194/amt-2019-318.

Schuster, G.L., Dubovik, O., Holben, B.N., 2006. Ångström exponent and bimodal aerosol size distributions. J. Geophys. Res. Atmos. 111 https://doi.org/10.1029/2005JD006328.

Su, T., Li, Z., Kahn, R., 2018. Relationships between the planetary boundary layer height and surface air pollutants derived from lidar observations over China: regional pattern and influencing factors. Atmos. Chem. Phys. 18 (21), 15921–15935. https://doi.org/10.5194/acp-18-15921-2018.

Su, T., Li, Z., Kahn, R., 2020. A new method to retrieve the diurnal variability of planetary boundary layer height from lidar under different thermodynamic stability conditions. Remote Sens. Environ. 237, 111519. https://doi.org/10.1016/j.rse.2019.111519.

Sun, L., Wei, J., Bilal, M., Tian, X., Jia, C., Guo, Y., Mi, X., 2016a. Aerosol optical depth retrieval over bright areas using Landsat 8 OLI images. Rem. Sens. 8 (1), 23. https://doi.org/10.3390/rs8010023.

Sun, L., Wei, J., Wang, J., Mi, X., Guo, Y., Lv, Y., Yang, Y., Gan, P., Zhou, X., Jia, C., Tian, X., 2016b. A universal dynamic threshold cloud detection algorithm (UDTCDA) supported by a prior surface reflectance database. J. Geophys. Res. Atmos. 121 (12), 7172–7196. https://doi.org/10.1002/2015JD024722.

Wei, J., Huang, B., Sun, L., Zhang, Z., Wang, L., Bilal, M., 2017. A simple and universal aerosol retrieval algorithm for Landsat series images over complex surfaces. J. Geophys. Res. Atmos. 122 (24), 13338–13355. https://doi.org/10.1002/2017JD026922.

Wei, J., Sun, L., 2017. Comparison and evaluation of different MODIS aerosol optical depth products over Beijing-Tianjin-Hebei region in China. IEEE J. Select. Top. Appl. Earth Obs. Rem. Sens. 10 (3), 835–844. https://doi.org/10.1109/JSTARS.2016.2595624.

Wei, J., Sun, L., Huang, B., Bilal, M., Zhang, Z., Wang, L., 2018a. Verification, improvement and application of aerosol optical depths in China. Part 1: inter-comparison of NPP-VIIRS and Aqua-MODIS. Atmos. Environ. 175, 221–233. https://doi.org/10.1016/j.atmosenv.2017.11.048.

Wei, J., Sun, L., Peng, Y., Wang, L., Zhang, Z., Bilal, M., Ma, Y., 2018b. An improved high-spatial-resolution aerosol retrieval algorithm for MODIS images over land. J. Geophys. Res. Atmos. 123 (12) https://doi.org/10.1029/2017JD027795, 291–12,307.

Wei, J., Huang, W., Li, Z., Xue, W., Peng, Y., Sun, L., Cribb, M., 2019a. Estimating 1-km-resolution PM$_{2.5}$ concentrations across China using the space-time random forest approach. Remote Sens. Environ. 231, 111221. https://doi.org/10.1016/j.rse.2019.111221.

Wei, J., Li, Z., Guo, J., Sun, L., Huang, W., Xue, W., Fan, T., Cribb, M., 2019b. Satellite-derived 1-km-resolution PM$_1$ concentrations from 2014 to 2018 across China. Environ. Sci. Technol. 53 (22), 13. https://doi.org/10.1021/acs.est.9b03258, 265–13,274.

Wei, J., Li, Z., Peng, Y., Sun, L., 2019c. MODIS Collection 6.1 aerosol optical depth products over land and ocean: validation and comparison. Atmos. Environ. 201, 428–440. https://doi.org/10.1016/j.atmosenv.2018.12.004.

Wei, J., Li, Z., Sun, L., Peng, Y., Wang, L., 2019d. Improved merge schemes for MODIS collection 6.1 dark target and deep blue combined aerosol products. Atmos. Environ. 202, 315–327. https://doi.org/10.1016/j.atmosenv.2019.01.016.

Wei, J., Peng, Y., Mahmood, R., Sun, L., Guo, J., 2019e. Intercomparison in spatial distributions and temporal trends derived from multi-source satellite aerosol products. Atmos. Chem. Phys. 19, 7183–7207. https://doi.org/10.5194/acp-19-7183-2019.

Wei, J., Li, Z., Peng, Y., Sun, L., Yan, X., 2019f. A regionally robust high-spatial-resolution aerosol retrieval algorithm for MODIS images over Eastern China. IEEE Trans. Geosci. Rem. Sens. 57 (7), 4748–4757. https://doi.org/10.1109/TGRS.2019.2892813.

Wei, J., Li, Z., Sun, L., Yang, Y., Zhao, C., Cai, Z., 2019g. Enhanced aerosol estimations from Suomi-NPP VIIRS images over heterogeneous surfaces. IEEE Trans. Geosci. Rem. Sens. 57 (12), 9534–9543. https://doi.org/10.1109/TGRS.2019.2927432.

Wei, J., Li, Z., Cribb, M., Huang, W., Xue, W., Sun, L., Guo, J., Peng, Y., Li, J., Lyapustin, A., Liu, L., Wu, H., Song, Y., 2020. Improved 1 km resolution $PM_{2.5}$ estimates across China using enhanced space-time extremely randomized trees. Atmos. Chem. Phys. 20 (6), 3273–3289. https://doi.org/10.5194/acp-20-3273-2020.

Xue, T., Zheng, Y., Tong, D., Zheng, B., Li, X., Zhu, T., Zhang, Q., 2019. Spatiotemporal continuous estimates of $PM_{2.5}$ concentrations in China, 2000–2016: a machine learning method with inputs from satellites, chemical transport model, and ground observations. Environ. Int. 123, 345–357. https://doi.org/10.1016/j.envint.2018.11.075.

Yu, H., Kaufman, Y.J., Chin, M., Feingold, G., Remer, L.A., Anderson, T.L., Balkanski, Y., Bellouin, N., Boucher, O., Christopher, S., DeCola, P., Kahn, R., Koch, D., Loeb, N., Reddy, M.S., Schulz, M., Takemura, T., Zhou, M., 2006. A review of measurement-based assessments of the aerosol direct radiative effect and forcing. Atmos. Chem. Phys. 6, 613–666. https://doi.org/10.5194/acp-6-613-2006.

Zeng, J., Yue, F., Wang, Z., Wu, Q., Qin, C., Li, S., 2019. Quantifying depression trapping effect on rainwater chemical composition during the rainy season in karst agricultural area, southwestern China. Atmos. Environ. 218, 116998. https://doi.org/10.1016/j.atmosenv.2019.116998.